Journal of Catalysis **194,** 14–22 (2000)
doi:10.1006/jcat.2000.2906, available online at http://www.idealibrary.com on IDEAL®

Nature of Spilt-over Hydrogen on Acid Sites in Zeolites: Observation of the Behavior of Adsorbed Pyridine on Zeolite Catalysts by Means of FTIR

Ryo Ueda, Toshiaki Kusakari, Keiichi Tomishige,[1] and Kaoru Fujimoto[1]

Department of Applied Chemistry, School of Engineering, The University of Tokyo, Hongo, Bunkyo-ku, Tokyo 113-8656, Japan

Received August 26, 1999; revised April 17, 2000; accepted April 25, 2000

The effect of spilt-over hydrogen on catalysts which were prepared by physically mixing zeolites or alumina with SiO_2-supported noble metals on chemisorbed pyridine was investigated by means of FTIR and TPD. It has been found that pyridine adsorbed on a Lewis acid site migrated to a Brønsted acid site under a hydrogen atmosphere. This suggests that spilt-over hydrogen should enhance the desorption of pyridine on the Lewis acid site, and that the possible state of spilt-over hydrogen on the Lewis acid site should be hydride, which has strong Lewis basicity. Furthermore, H–D exchange ($–OH + D_2$) of the Brønsted acid site was also carried out, which leads to a complete description of interactions between spilt-over hydrogen and acid sites of zeolite. © 2000 Academic Press

Key Words: **hydrogen spillover; zeolite; hybrid catalyst; Brønsted and Lewis acid sites; pyridine migration; proton and hydride.**

INTRODUCTION

Spilt-over hydrogen is known to have a strong effect on the catalytic reaction system on solid acid catalysts. Our group found that the catalyst prepared by the physical mixture of Pt/SiO_2 and H–ZSM-5 (denoted as "hybrid catalyst") was very effective for the hydroisomerization or the hydrocracking of *n*-pentane, *n*-hexane, and other paraffinic hydrocarbons under a hydrogen atmosphere (1–5). We concluded that both high conversion and high selectivity were due to the effect of hydrogen spillover, and suggested that spilt-over hydrogen has two forms, H^+ and H^-. It is suggested that spilt-over H^+ regenerates a Brønsted acid site which is consumed by the reaction between paraffin and proton to form the carbenium ion and hydrogen. Spilt-over H^- stabilizes the carbenium ion intermediate resulting from the hydrogenation before its desorption as olefin. This model is rather in contrast to the conventional bifunctional reaction mechanism (6–8). Shishido and Hattori pointed out that hydrogen promoted the activity of cumene cracking over $Pt/SO_4^{2-}–ZrO_2$ and inhibited its deactivation. It is expected that the Brønsted acid site generated from spilt-over hydrogen acts as the active site for the catalytic reaction (9). Hosoi *et al.* found that when $Pt/SO_4^{2-}–ZrO_2$ catalyst was used for skeletal isomerization of *n*-pentane in the presence of hydrogen, it showed not only high activity but also persistence of the activity for a long period, more than 1000 h. They explained that the hydrogen had an effect on the removal of coke formed during the reaction by hydrogenating it (10). It has been reported that spillover of hydrogen occurs even when the physical mixture of supported metal catalyst and zeolite is exposed to a hydrogen atmosphere (11). A hydrogen molecule in the gas phase is dissociated first on the metal surface to atomic hydrogen and then migrates onto the support surface, and further, onto the surface of adjacent zeolite particles.

There has been a lot of discussion so far about the nature of spilt-over hydrogen species, such as H atoms, radicals, H^+ and H^- ions, ion pairs, H_3^+ species or protons, and electrons (12, 13). Protons formed from spilt-over hydrogen are suggested to act as catalytic active sites for an acid-catalyzed reaction (14–16). The present authors have pointed out the possibility of the participation of H^+ and H^- which are produced from spilt-over hydrogen in the hydroisomerization or hydrocracking of aliphatic hydrocarbons over Pt and Pd-supported zeolites or a physically mixed $Pt/SiO_2 +$ protonic zeolite system (1, 5, 17). Roland *et al.* have given a clear proof for the electrical charge of the spilt-over species, which was obtained through H–D exchange studies on the influence of a homogeneous magnetic field. The migration of spilt-over hydrogen (deuterium) in the Pt/NaY–HNaY catalyst was hindered, which was attributed to the influence of the Lorentz force on the electrically charged moving particles (18, 19), while there is assumed to be an equilibrium between protons and radicals as spilt-over hydrogen species (20). Thus, the elucidation of the nature of spilt-over hydrogen species is a matter of deep interest.

One of hydrogen effects in hydrocarbon conversion on solid acid catalysts is to inhibit catalyst deactivation. The

---

[1] To whom correspondence should be addressed. Fax: +81-3-5841-8578. E-mail: tomi@appchem.t.u-tokyo.ac.jp.

0021-9517/00 $35.00

deactivation of zeolite related to its acidity and pore structure has attracted much attention (21). Carbonaceous deposits (coke) are the principal cause of zeolite deactivation in the process of hydrocarbon conversions, and the adsorption of coke precursor on the acid sites is one of the factors which trigger the formation and growth of coke. We believe that our study can contribute to the elucidation of the hydrogen effect in this problem.

Pyridine is a typical organic base and is chemisorbed on both Brønsted (B) and Lewis (L) acid sites on zeolite catalysts while pyridinium ion and coordinately bonded pyridine complexes are formed on B and L sites, respectively, giving different IR adsorption bands on each occasion (22–24). Zhang *et al.* have found by FTIR that pyridine strongly adsorbed on acid sites of H–ZSM-5 was hydrogenated over Pt/H–ZSM-5 and $Pt/SiO_2 +$ H–ZSM-5 hybrid catalyst to adsorbed piperidine in the presence of gaseous hydrogen at around 473 K. It is claimed that the phenomena revealed the occurrence of hydrogen spillover from Pt sites to acid sites of zeolite (25, 26). Fan *et al.* reported that this hydrogenation rate was dependent not only on the nature of supported metals in the hybrid catalyst system but also on the acidic strength of the zeolite catalysts (27).

We have investigated the effect of hydrogen spillover over a $Pd/SiO_2 +$ H–USY hybrid catalyst on pyridine chemisorbed on the Lewis acid site of an H–USY zeolite by means of FTIR, and have pointed out the possibility of spilt-over hydrogen enhancing the desorption of pyridine adsorbed on the L site (28). In this paper, we are going to discuss in more detail this new concept of the behavior of spilt-over hydrogen interacting with the Lewis acid site and the mechanism of hydrogenation of adsorbed pyridine. Furthermore, we will also discuss the interaction between spilt-over hydrogen and the Brønsted acid site by means of the exchange reaction between D_2 and –OH.

EXPERIMENTAL

Catalyst Preparation

Pd/SiO_2 was prepared by impregnating a commercially available SiO_2 (Aerosil 380) with an aqueous solution of $PdCl_2$ (Soekawa Chemicals, Pd 59%). A dilute aqueous solution of HCl was added to make $PdCl_2$ more soluble in water. After impregnation and the removal of water, the sample was dried at 393 K for 12 h, and was calcined at 723 K in air for 3 h. The loading of Pd was 2.5 wt%. The Pd–USY hybrid catalyst was prepared by cogrinding the mixture of Pd/SiO_2 and H–USY (Tosoh Co., HSZ-330HUA, $SiO_2/Al_2O_3 = 6.3$) for 30 min. The weight ratios used in this study were Pd/SiO_2 : H–USY = 1 : 19 as for the Pd–USY hybrid catalyst. Pd–USY (1 : 9 and 1 : 4) was also used in the experiment to determine the dependence on the Pd/SiO_2 concentration. Supported metal catalysts Pt/SiO_2, Rh/SiO_2, and Ir/SiO_2 were also prepared by a similar impregnation procedure using $H_2PtCl_6 \cdot 6H_2O$ (Soekawa Chemicals, Pt 37%), $RhCl_3 \cdot 3H_2O$ (Soekawa Chemicals, Rh 39%), and $IrCl_3 \cdot nH_2O$ (Soekawa Chemicals, Ir 59%) as metal precursors, respectively. These catalysts were used to prepare Pt–USY, Rh–USY, and Ir–USY hybrid catalysts. H–mordenite (Tosoh Co., JRC-Z-HM20, $SiO_2/Al_2O_3 = 18.9$), H–beta (Zeolist Int., CBV-811B, $SiO_2/Al_2O_3 = 22$), H–ZSM-5 (Tosoh Co., HSZ-840HOA, $SiO_2/Al_2O_3 = 44$), and γ-Al_2O_3 (Aerosil aluminum oxide C) were used to prepare Pd–mordenite, Pd–beta, Pd–ZSM-5, and Pd–Al_2O_3 hybrid catalysts. In addition, supported Pd/USY (0.5 and 5.0 wt% loading) catalyst was prepared using $Pd(NH_3)_4Cl_2 \cdot H_2O$ (Soekawa Chemicals, Pd 40%) and H–USY. Pd was introduced by the ion-exchange method with an aqueous solution of $Pd(NH_3)_4Cl_2 \cdot H_2O$. Ion exchange was carried out under stirring at 353 K for 6 h, and Pd/USY products were washed with water until no chrolide ion was detected. Then, the samples were dried at 393 K for 12 h, and calcined at 723 K in air for 3 h.

Pyridine Chemisorption and the Introduction of H_2 (and D_2)

Pyridine chemisorption and the introduction of H_2 gas on the hybrid catalysts were carried out in a quartz *in situ* IR cell with CaF_2 windows connected to the vacuum-closed circulating system and the atmospheric gas flow system. All samples were pressed into a self-supporting water (pressure, 400 kg/cm^2) with a diameter of 10 mm and a weight of about 10 mg. The samples were reduced by flowing H_2 at 673 K for 1 h and outgassed *in vacuo* at 773 K for 1 h as the pretreatment procedure. Then the samples were exposed to 1.0 kPa vapor of pyridine (Nakalai tesque, 99.5%) at 423 K for 30 min, followed by evacuation at 423 K for 30 min in order to remove gaseous and weakly adsorbed pyridine. In this paper, the coverage of pyridine after this evacuation at 423 K is defined as saturate coverage. In order to control the coverage of pyridine adsorption on acid sites, additional evacuation at higher temperature was carried out. Hydrogen gas was introduced into the pyridine-preadsorbed samples at 423 K. The flow rate of the gas was 15 ml/min.

FTIR spectra were obtained by PROTÉGÉ 460 (Nicolet) with an MCT detector. Coverage on the Brønsted (B) and Lewis (L) acid sites by pyridine was estimated from the ratio of the peak area (B, 1540 cm^{-1}; L, 1450 cm^{-1}) to its saturation. Since the peak of piperidine overlapped the peak of pyridine adsorbed on the Lewis acid site, subtraction of the spectra was used for estimation of the coverage of the Lewis acid site. In the subtraction of the contribution of adsorbed piperidine, the subtraction factor was determined on the basis of the 1475 cm^{-1} peak, which is clearly different from the peaks due to adsorbed pyridine. All the spectra were measured at 423 K.

In several experiments, D_2 (Isotec Inc., 99.8%) was used as the flow gas instead of H_2 in order to observe the exchange reaction between D_2 and –OH.

RESULTS AND DISCUSSION

Promoting Effect of Hydrogen Spillover on Pyridine Migration Adsorbed on a Lewis Acid Site in USY Zeolite

Figure 1 shows the change in the FTIR spectra when hydrogen gas was introduced into the sample on which pyridine was adsorbed at the saturation level. The peak at 1450 cm^{-1} (denoted as the L peak) is attributed to pyridine on the L acid site of zeolite, while the 1540 cm^{-1} peak (denoted as the B peak) is attributed to pyridine on the B site (22–24). Both the B and L peaks decreased with time on stream of hydrogen. On the other hand, new peaks around 1460 and 1475 cm^{-1} appeared. Spectrum e in Fig. 1 is similar to that of chemisorbed piperidine (25). Under these conditions, it seems that pyridine on both the B and L sites was hydrogenated into piperidine simultaneously by spilt-over hydrogen supplied to each acid site, as was claimed by Zhang *et al.* (25–27). However, the hydrogenation turned out to have multiple steps as described below. The site of piperidine adsorption did not influence the FTIR spectrum. The ratio of peak intensities was almost the same on all the various zeolite catalysts used in this paper.

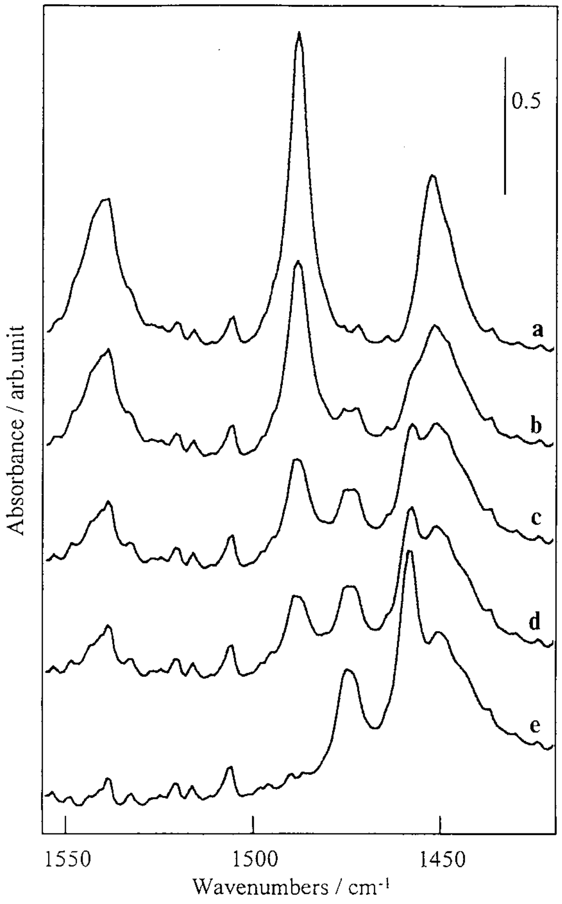

FIG. 1. FTIR spectra of pyridine adsorbed on $Pd/SiO_2 +$ H–USY hybrid catalyst at saturated coverage. (a) Evacuation at 423 K, (b) 20 min, (c) 40 min, (d) 50 min, and (e) 90 min (b to e, time on stream of H_2). Condition of H_2 flow: 423 K, 15 ml/min, pure H_2. Initial coverage of pyridine: B 100%, L 100%. Pyridine adsorption temperature: 423 K.

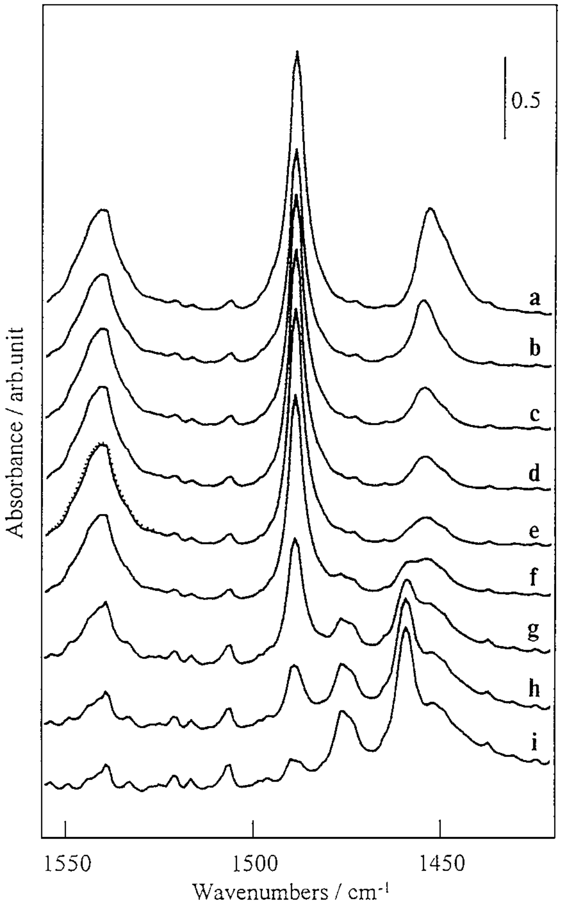

FIG. 2. FTIR spectra of pyridine adsorbed on $Pd/SiO_2 +$ H–USY hybrid catalyst at medium coverage. (a) Evacuation at 423 K for 0.5 h, (b) evacuation at 598 K for 0.5 h, (c) 5 min, (d) 10 min, (e) 30 min, (f) 90 min, (g) 180 min, (h) 270 min, and (i) 360 min (c to i, time on stream of H_2). Condition of H_2 flow: 423 K, 15 ml/min, pure H_2. Initial coverage of pyridine: B 85%, L 50%. Pyridine adsorption temperature: 423 K. Dotted line represents the saturation of B site.

Figure 2 shows the change in the IR spectra when hydrogen gas was introduced into the sample on which pyridine was adsorbed at medium coverage. In this case, the sample was evacuated at 598 K for 30 min after pyridine adsorption. The amounts of pyridine left on the B and L sites were 85% and 50% of the saturated amount, respectively (Fig. 2b). At the initial stage, the L peak decreased and the B peak increased with time on stream without growth of the piperidine peak. When the B peak reached the saturation level, piperidine began to be formed. The result indicates

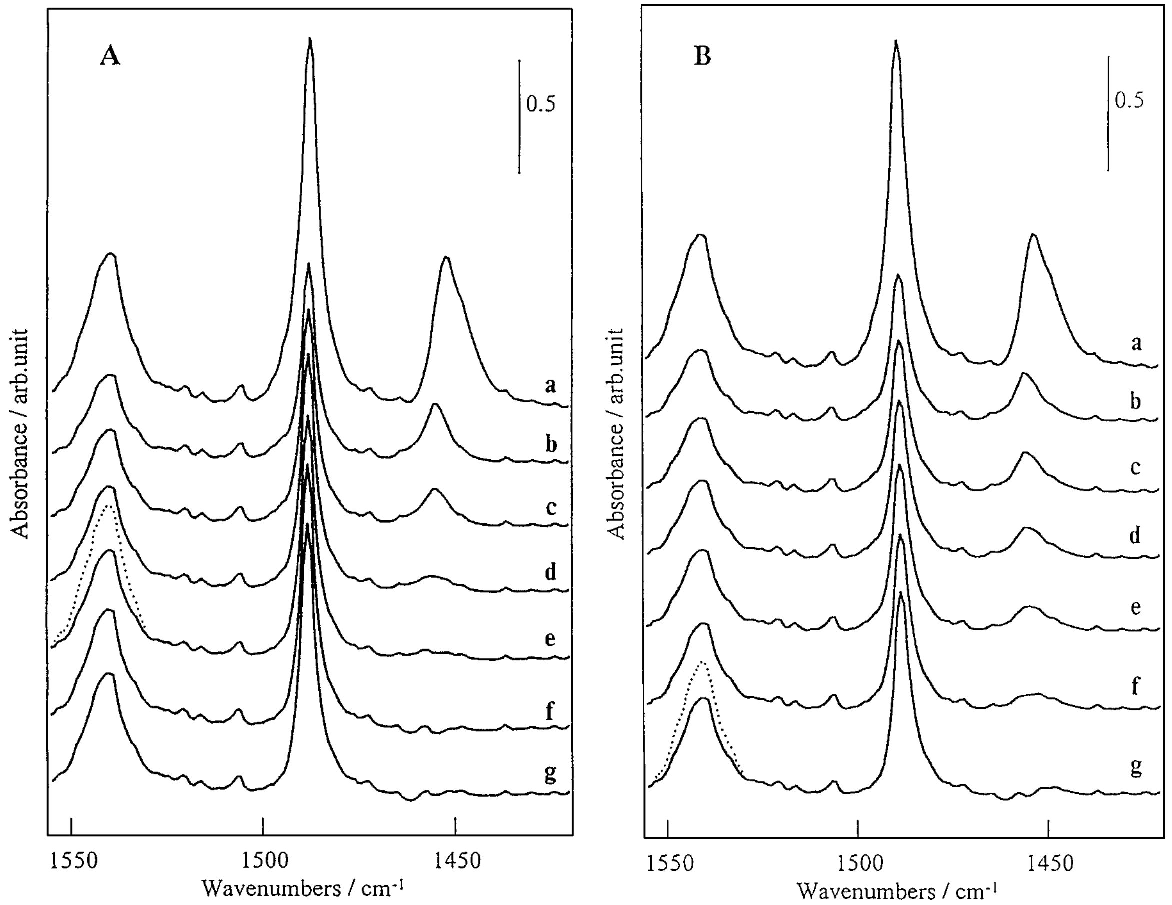

FIG. 3. FTIR spectra of pyridine adsorbed on Pd/SiO_2 + H–USY (1 : 19) hybrid catalyst (A) and H–USY (B) at low coverage. (a) Evacuation at 423 K for 0.5 h, (b) evacuation at 698 K for 0.5 h, (c) 1 min, (d) 2 min, (e) 3 min, (f) 15 min, and (g) 150 min (c to g, time on stream of H_2). Condition of H_2 flow: 423 K, 15 ml/min, pure H_2. Initial coverage of pyridine: B 55%, L 25% (A); B 60%, L 28% (B). Dotted line represents the saturation of B site.

that pyridine adsorbed on the L acid site migrates to the B site until its saturation, and after that the hydrogenation of pyridine starts.

Figure 3A shows the change in the IR spectra of the sample with low coverage of pyridine, 55% B site and 25% L site. These spectra indicate that pyridine migrated from the L site to the B site. Under these conditions, all of the residual pyridine adsorbed on the L site migrated to the B site. After that, there was still vacant B site since the total pyridine coverage at the initial stage did not reach saturation of the B site. The peak of hydrogenated product was not observed for 150 min or more. This means that the hydrogenation did not occur on the acid sites of the zeolite and that pyridine is likely to be converted into piperidine on metal surfaces with gaseous hydrogen.

In order to clarify the effect of spilt-over hydrogen on the migration of pyridine from the Lewis site to the Brønsted site, we investigated the behavior of pyridine migration over the H–USY catalyst (Fig. 3B). It is difficult to form spilt-over hydrogen, as shown in Fig. 9, on this catalyst. However, the phenomenon of pyridine migration was also observed. This may be caused by the gas-phase molecule. This phenomenon was observed in the case of the inert gas flowing (He and N_2), and the migration rate was almost the same in all cases. The mechanism is not clear at present. The migration rates on two catalysts are compared.

In Fig. 4, pyridine coverage on the L site and the B site as a function of time on stream is shown under each condition. Pyridine coverage on the L site was decreased and that on the B site was increased correspondingly with time on stream. It is estimated that the rate of pyridine migration on the hybrid catalyst system was about 2.5 times higher than that on the H–USY catalyst. This indicated that spilt-over hydrogen from the supported metal catalyst to the zeolite enhances the desorption of pyridine on the L site, and thus plays an important role in pyridine hydrogenation.

Based on the above results, it is suggested that spilt-over hydrogen has the stronger interaction with Lewis acid site, and that one of the species of spilt-over hydrogen is the H^- type which has higher basicity. Considering the charge balance, coexistence of H^+ is expected, but it cannot be identified by this kind of experiment. As for H^+, we carried out a successful FTIR observation of the interaction between spilt-over hydrogen and the Brønsted acid site using D_2, as

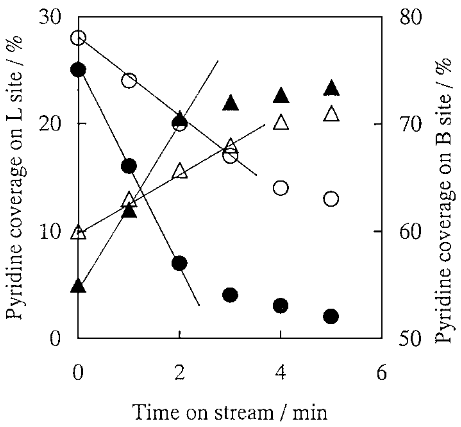

FIG. 4. Pyridine coverage on L site (●, ○) and B site (▲, △) as a function of time on stream. Pd/SiO$_2$ + H–USY (1 : 19) hybrid (●, ▲); H–USY (○, △). Condition of H$_2$ introduction: 423 K, 15 ml/min, pure H$_2$. Initial coverage of pyridine: B 55% and L 25% (Pd/SiO$_2$ + H–USY); B 60% and L 28% (H–USY). Pyridine adsorption temperature: 423 K. Evacuation: 698 K for 0.5 h.

mentioned later. Here, we propose a reaction mechanism for hydrogenation of pyridine chemisorbed on acidic sites of H–USY in a hybrid catalyst system. The scheme is shown in Fig. 5. First, the pyridine on the L acid site of the zeolite is desorbed, and moves to the vacant B site until its saturation (Fig. 5a). Then, after saturation of the B site, excess pyridine from the L site moves to the metal surface and is hydrogenated into piperidine (Fig. 5b). As piperidine has a higher basicity than pyridine, the exchange of piperidine with pyridine on both acid sites occurs easily, and thus the reaction continues until all of the pyridine on the acid sites is converted into piperidine. The transportation of pyridine in this reaction is supposed to be surface diffusion, as the total amount of pyridine (and piperidine) was sustained during the whole reaction.

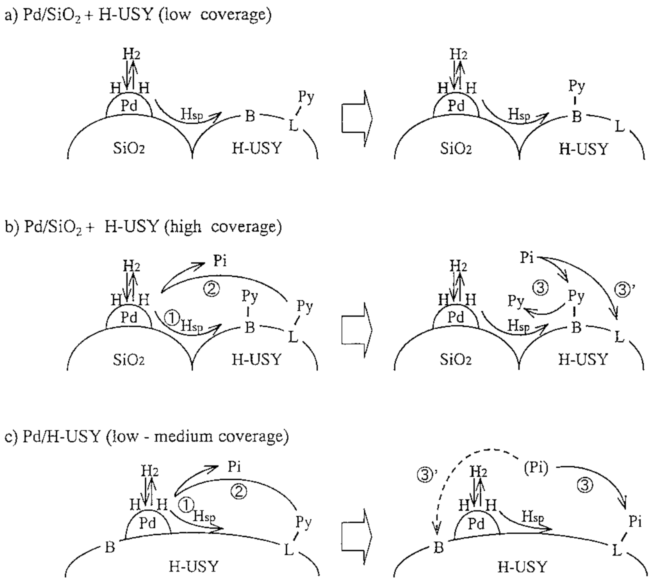

FIG. 5. Proposed schematic of migration of pyridine chemisorbed on Brønsted and Lewis acid sites of zeolite promoted by hydrogen spillover effect (a) and hydrogenation of pyridine in Pd/SiO$_2$ + H–USY hybrid catalyst system (b). Application of the schematic to Pd/H–USY catalyst (c). Py, pyridine (C_5H_5N); Pi, piperidine ($C_5H_{11}N$); H$_{sp}$, spilt-over hydrogen.

A similar spectroscopic study was carried out using different catalyst systems. Figure 6 shows the change in the IR spectra when hydrogen gas was introduced onto a supported Pd/USY (0.5 wt% loading) catalyst on which pyridine adsorbed at medium coverage. The sample had been evacuated at 598 K for 30 min after pyridine adsorption. The amounts of pyridine left on the B and L sites were 80% and 50% of the saturated amount, respectively (Fig. 6b). In this case, the behavior of the peaks was similar to that of the hybrid catalyst peaks. The L peak decreased and the B peak increased before the beginning of the hydrogenation, which suggests the migration of pyridine. Figure 7 shows

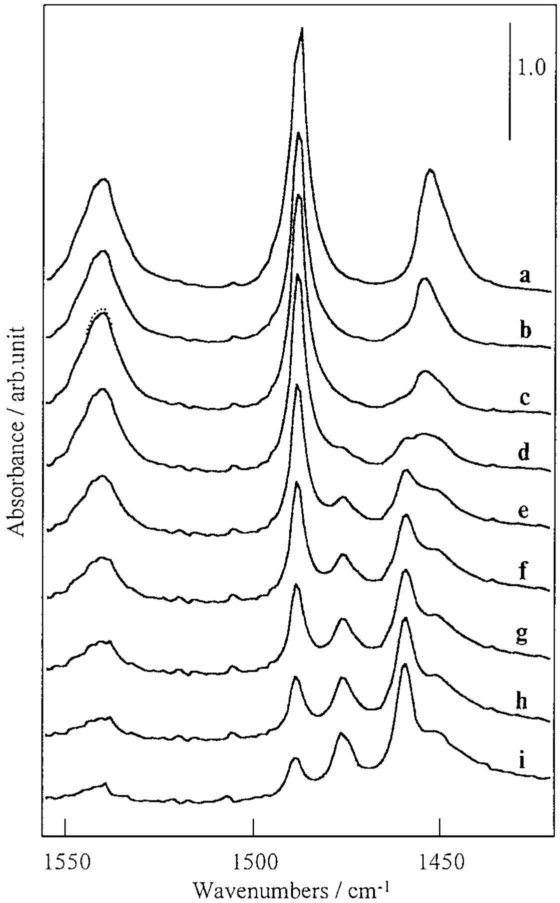

FIG. 6. FTIR spectra of pyridine adsorbed on Pd/H–USY (0.5 wt% Pd supported) catalyst at medium coverage. (a) Evacuation at 423 K for 0.5 h, (b) evacuation at 598 K for 0.5 h, (c) 1 min, (d) 3 min, (e) 5 min, (f) 10 min, (g) 15 min, (h) 30 min, and (i) 60 min (c to i, time on stream of H$_2$). Condition of H$_2$ flow: 423 K, 15 ml/min, pure H$_2$. Initial coverage of pyridine: B 80%, L 50%. Pyridine adsorption temperature: 423 K. Dotted line represents the saturation of B site.

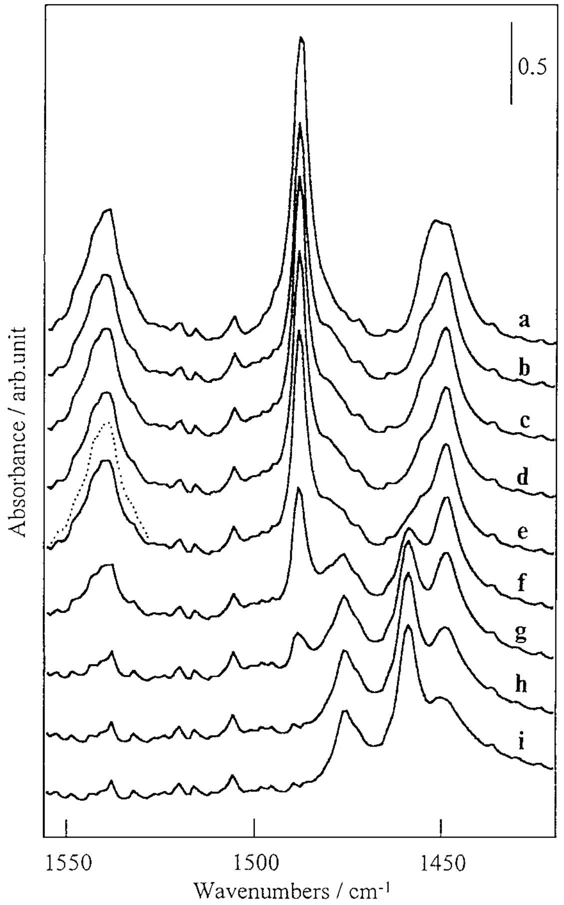

FIG. 7. FTIR spectra of pyridine adsorbed on Pd/H–USY (5 wt% Pd supported) catalyst at medium coverage. (a) Evacuation at 423 K for 0.5 h, (b) evacuation at 598 K for 0.5 h, (c) 1 min, (d) 3 min, (e) 5 min, (f) 10 min, (g) 15 min, (h) 30 min, and (i) 60 min (c to i, time on stream of H_2). Condition of H_2 flow: 423 K, 15 ml/min, pure H_2. Initial coverage of pyridine: B 85%, L 75%. Pyridine adsorption temperature: 423 K. Dotted line represents the saturation of B site.

the change in the IR spectra when hydrogen gas was introduced onto supported Pd/USY (5 wt% loading) catalyst on which pyridine adsorbed at medium coverage. The sample had been evacuated at 598 K for 30 min after pyridine adsorption. The amounts of pyridine left on the B and L sites were 85% and 75% of the saturated amount, respectively (Fig. 7b). In this case, the behavior of the peaks was quite different from that on a hybrid catalyst or a low metal loading catalyst. Peak changes which suggest the migration of pyridine prior to hydrogenation were not observed. Hydrogenation began without saturation of the B site. Application of the proposed mechanism to the supported metal catalyst system is shown in Fig. 5c. The model scheme suggests that when metal concentration is high in the zeolite particle, adsorbed pyridine can easily be hydrogenated into piperidine during the migration from the L site to the B site, and that saturation of the B site is not necessary for the beginning of the hydrogenation. The proximity between Pd and acid sites enables hydrogenation to occur without saturation of the B site. This explains the results very well.

Effect of the Kinds of Zeolites on Migration of Adsorbed Pyridine

A promoting effect of hydrogen spillover on pyridine migration adsorbed on a Lewis acid site of a zeolite was observed in the Pd–USY hybrid catalyst system. We also carried out similar experiments using H–mordenite, H–beta, and H–ZSM-5. The results are shown in Table 1. The effect of spilt-over hydrogen on desorption of adsorbed pyridine on the L site can be estimated from the ratio {(migration rate in Pd–zeolite)/(migration rate in zeolite)}. The weight ratios of hybrid catalysts are as follows: Pd/SiO_2 : H–mordenite = 1 : 49, Pd/SiO_2 : H–beta = 1 : 49, and Pd/SiO_2 : H–ZSM5 = 1 : 99. The data listed in Table 1 show that the effect can be seen not only in H–USY but also in H–mordenite and H–beta. However, no

TABLE 1

Effect of Spilt-over Hydrogen on Migration Rate of Pyridine Adsorbed on Lewis Acid Site in Various Zeolites

Catalyst	Evacuation temp[a]/K	Initial coverage /%		Migration rate of pyridine on L acid site [b]/% · min	Ratio of migration rate Pd–zeolite/ zeolite
		B	L		
Pd–USY	698	55	25	9.3	
USY	698	60	28	3.7	2.5
Pd–morenite	773	45	30	7.5	
Mordenite	773	30	35	4.2	1.8
Pd–beta	773	45	70	9.6	
Beta	773	40	65	5.1	1.9
Pd–ZSM-5	723	80	45	7.4	
ZSM-5	773	60	35	8.6	0.9

[a] Pyridine adsorption temperature was 423 K for all the samples.

[b] Condition of H_2 flow: 423 K, 15 ml/min, pure H_2.

TABLE 2

Properties of Supported Metal Catalysts

Catalyst	Metal loading wt%	Metal loading $\mu mol \cdot g\text{-}cat^{-1}$	Amount of H_2 adsorption[a]/ $\mu mol \cdot g\text{-}cat^{-1}$	Dispersion[b]
Pd/SiO_2	2.5	235	44.7	0.38
Pt/SiO_2	2.5	128	13.4	0.21
Rh/SiO_2	2.5	243	41.3	0.34
Ir/SiO_2	2.5	130	11.7	0.18

[a] Amount of H_2 adsorption on the sample reduced at 673 K and evacuated at 773 K was measured by volumetric method at room temperature.
[b] $H/M_s = 1$ was assumed.

difference in the migration rate between the Pd–ZSM-5 hybrid catalyst and H–ZSM-5 was observed. Since H–ZSM-5 has a relatively strong acidity and a small pore size, the migration rate may be limited by the diffusion of pyridine.

Effect of the Kinds and Amounts of Supported Metal Catalysts on Migration of Adsorbed Pyridine

In addition to the Pd/SiO_2 catalyst, Pt/SiO_2, Rh/SiO_2, and Ir/SiO_2 were also used in hybrid catalysts to investigate the effect of the kinds of metal on the migration rate. The properties of these catalysts are listed in Table 2. In Fig. 8, pyridine coverage on the L site as a function of reaction time on Pd–USY, Pt–USY, Rh–USY, and Ir–USY hybrid catalyst systems is shown. The weight ratio was determined as follows: supported metal catalyst (2.5 wt%) : H–USY = 1 : 19. The initial coverage of pyridine on the samples was about 55% of the saturated amount. The result suggests that pyridine migration rates do not depend on the kinds of metal in hybrid catalysts from which hydrogen spills-over onto zeolites. The amounts of metal in the hybrid catalysts were also varied by changing the weight ratios [Pd/SiO_2 (2.5 wt%) : H–USY = 1 : 19, 1 : 9, and 1 : 4], but the pyridine migration rate did not seem to be influenced by the amount of metal. Judging from these results, there could be two interpretations: (1) the zeolite is saturated with spilt-over hydrogen even for low metal concentrations or (2) the number of H^- is limited even when the total H concentration increases.

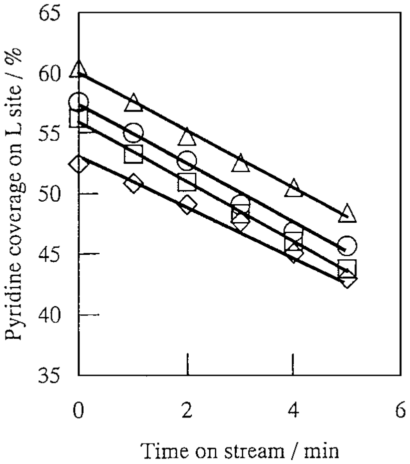

FIG. 8. Effect of the kinds of metal on pyridine migration rate. (○) $Pd/SiO_2 + H$–USY hybrid catalyst (Pd/SiO_2 : H–USY = 1 : 19); (△) $Pt/SiO_2 + H$–USY hybrid catalyst (Pt/SiO_2 : H–USY = 1 : 19); (□) $Rh/SiO_2 +$ H–USY hybrid catalyst (Rh/SiO_2 : H–USY = 1 : 19); (◇) $Ir/SiO_2 +$ H–USY hybrid catalyst (Ir/SiO_2 : H–USY = 1 : 19). Condition of H_2 flow: 423 K, 15 ml/min, pure H_2. Initial coverage of pyridine on L site: around 60%. Pyridine adsorption: 423 K. Evacuation: 598 K for 0.5 h.

Exchange Properties between Brønsted Acid Site and Spilt-over Hydrogen

We have focused on the interaction between spilt-over hydrogen and the Lewis and site so far. Now we are going to discuss the interaction between spilt-over hydrogen and the Brønsted acid site. By using D_2 instead of H_2, we could observe the H–D exchange reactions of Brønsted–OH and pyridine adsorbed on the B site. Figure 9 shows

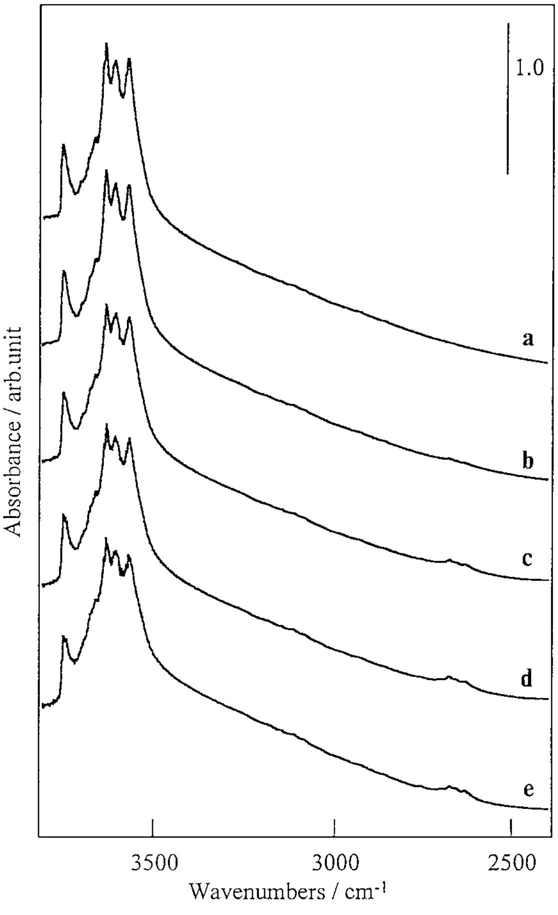

FIG. 9. FTIR spectra of Brønsted–OH and –OD in H–USY catalyst. (a) Before D_2 introduction, (b) 10 min, (c) 20 min, (d) 30 min, and (e) 60 min (b to e, time on stream of D_2). Condition of D_2 flow: 423 K, 15 ml/min pure D_2.

the change in the FTIR spectra when deuterium gas was introduced onto H–USY. Peaks around 3600 cm^{-1} denoted as B–OH peaks (3560, 3600, and 3625 cm^{-1}) are attributed to protonic Brønsted–OH in zeolite H–USY, while peaks around 2650 cm^{-1} denoted as B–OD peaks (2630, 2655, and 2670 cm^{-1}) are attributed to Brønsted–OD generated by the H–D exchange reaction (29). Figure 10 shows the change in the FTIR spectra when D_2 gas was introduced onto the Pd–USY hybrid catalyst. The exchange rate on the Pd–USY hybrid catalyst was almost 100 times as fast as that on H–USY. The result indicates that when hydrogen spillover occurs, the change of B–OH into B–OD is drastically promoted. It is clear that there is also a strong interaction between spilt-over hydrogen and the Brønsted acid site. In addition, it is found from Fig. 10 that the peak at 3740 cm^{-1} hardly decreased during the reaction. This peak is attributed to isolated silanol–OH which has weak acidity. It is suggested that the strength of the acid site greatly influences the rate of exchange. Taking this into consideration, the change of the peak at 3600 cm^{-1} into 2655 cm^{-1} seems to be slightly slower than those of the other two peaks at 3560 and 3625 cm^{-1}, which is expected to be due to the difference in the acidic strength of each B site.

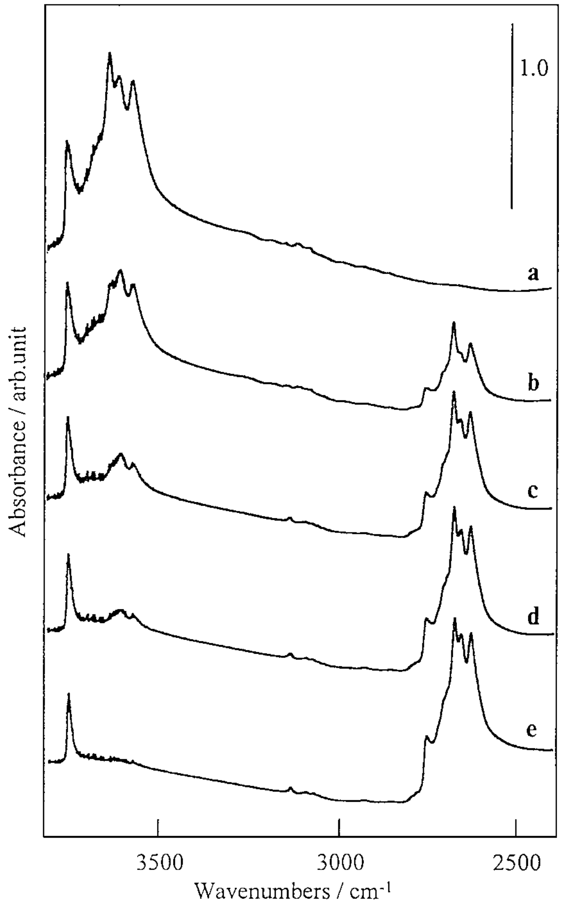

FIG. 10. FTIR spectra of Brønsted–OH and –OD in $Pd/SiO_2 + H$–USY (1:19) hybrid catalyst. (a) Before D_2 introduction, (b) 1 min, (c) 5 min, (d) 10 min, and (e) 30 min (b to e, time on stream of D_2). Condition of D_2 flow: 423 K, 15 ml/min pure D_2.

We also measured FTIR spectra when D_2 was introduced onto the Pd–USY sample with adsorbed pyridine. Prior to D_2 introduction, the sample had been kept under an H_2 flow for 30 min to shift most of the pyridine onto the B site. Pyridine adsorbed on acid sites just before D_2 introduction was B 80% and L 20% of the saturated amount, respectively. With the introduction of D_2, the B peak decreased and finally disappeared. This means that the pyridinium ion $C_5H_5NH^+$ adsorbed on the Brønsted acid site was converted into $C_5H_5ND^+$ by spilt-over hydrogen. This result clearly indicates the interaction between spilt-over hydrogen and adsorbed species on the B acid site.

Reactivity of Spilt-over Hydrogen (Deuterium) Supplied on Zeolite Surface with Brønsted and Lewis Acid Sites

Based on the results above, we discussed the reactivity of spilt-over hydrogen (deuterium) with Brønsted and Lewis acid sites. As for the rate of supply of spilt-over $H_2(D_2)$ onto the zeolite surface, we estimated it from B–OH changing into B–OD. As for the rate of interaction between spilt-over $H_2(D_2)$ and the B site, we estimated it from $C_5H_5NH^+$ changing into $C_5H_5ND^+$. As for the rate of interaction between spilt-over $H_2(D_2)$, we estimated it from desorption and migration of C_5H_5N from the L site. We made a comparison among these three rates. It was estimated that the initial rate of supply of spilt-over D_2 onto the zeolite surface (R_Z) was about 3000 μmol · g-cat^{-1} min^{-1} from the result in Fig. 10. The rates of interaction were about 600 μmol · g-cat^{-1} min^{-1} with the B site (R_B) from the result of H–D exchange under pyridine adsorption. The rate of pyridine migration was about 40 μmol · g-cat^{-1} min^{-1} with the L site (R_L) from the results of Fig. 3A. We can consider several reaction paths for interactions between spilt-over hydrogen (deuterium) and B or L acid sites as follows.

$$D_2 \rightarrow 2D^{\bullet} \quad [1a]$$

$$D^{\bullet} \rightarrow D^+ + e^- \quad [1b]$$

$$D^{\bullet} + e^- \rightarrow D^- \quad [1c]$$

$$BO^- \cdots H^+ + D^{\bullet} \rightarrow BO^- \cdots D^+ + H^{\bullet} \quad [2a]$$

$$BO^- \cdots H^+ + D^+ \rightarrow BO^- \cdots D^+ + H^+ \quad [2b]$$

$$D^- + L \rightarrow L \cdots D^- \quad [3]$$

The dissociation of D_2 on the metal surface corresponds to [1a]. D radical can be converted to D^+ if reaction [1b] proceeds, and then D^- can be formed by the interaction of radical and electron [1c]. It is possible that radical [2a] and D^+ [2b] exchange with the B site. D^- can interact with the L site.

On the basis of the scheme, R_B and R_L correspond to reaction [1a] + [2a] + [2b] and [1a] + [1c] + [3], respectively. The fact $R_B \gg R_L$ suggests that the interaction of D with the B site is much faster than that with the L site, which seems to correspond well with reaction [2a] being faster than [1c] + [3], since the former is single-stepped while the latter is multi-stepped. Considering the charge balance of the total system, the concentration of D^+ is equal to that of $D^- + e^-$. The possibility of reaction of these species with acid sites is high enough, so that the reaction rate can reflect the concentration. Therefore, our results suggest that the radical species might be richer than D^+ and D^- on the catalyst surface. Another explanation of $R_B \gg R_L$ is that the H–D exchange reaction can proceed without disturbance of charge balance described in [2a] when we assume the reactive exchange. We expect that such results will be an important clue to a detailed clarification of the nature and behavior of spilt-over hydrogen species on zeolites and other solid acid surfaces. This study will also contribute to our understanding of the mechanism of removal of poisoning materials on solid acid catalysts via hydrogen spillover phenomenon.

CONCLUSION

FTIR measurement of the behavior of chemisorbed pyridine on Brønsted and Lewis acid sites of zeolites in the Pd/SiO_2 + H–USY hybrid catalyst system under a hydrogen atmosphere was carried out. We observed that migration of pyridine from the Lewis acid site to the Brønsted acid site was drastically promoted by the hydrogen spillover effect. It is suggested that spilt-over hydrogen has a function of enhancing desorption of pyridine adsorbed on the Lewis acid site, and thus it is expected to be supplied to the Lewis acid site in the possible form of hydride ion (H^-). A similar phenomenon was also observed in other zeolites. Since neither the kind nor the amount of metal influenced the migration rate, the supply of spilt-over hydrogen on desorption of pyridine adsorbed on the L site seems to saturate with only a small amount of metal.

Spilt-over hydrogen supplied onto a zeolite surface interacts not only with the L site but also with the B site. This was confirmed by using a deuterium (D_2) atmosphere instead of hydrogen. The change of Brønsted–OH into OD was drastically promoted by the existence of spilt-over deuterium. Pyridinium ion $C_5H_5NH^+$ adsorbed on the B site was also easily converted into $C_5H_5ND^+$ with spilt-over deutrium. Considering the charge balance, an assumption that H^+ (D^+) coexists with H^- (D^-) on the zeolite surface may be appropriate. However, since we found that the interaction of spilt-over deutrium with the B site was much faster than that with the L site, spilt-over hydrogen seems to be supplied to the B site in radical-like and protonic forms.

What is most important in our study is the discovery that the desorption of basic molecules on Lewis acid sites is promoted by spilt-over hydrogen, probably by hydride ion. This seems to correlate that hydrogen spillover has some effect on the inhibition of poisoning acid sites in various catalytic reactions.

REFERENCES

1. Fujimoto, K., Maeda, K., and Aimoto, K., *Appl. Catal. A General* **91**, 81 (1992).
2. Nakamura, I., Sunada, K., and Fujimoto, K., *Stud. Surf. Sci. Catal.* **105**, 1005 (1997).
3. Nakamura, I., Sunada, K., and Fujimoto, K., *Stud. Surf. Sci. Catal.* **106**, 361 (1997).
4. Zhang, A., Nakamura, I., and Fujimoto, K., *Stud. Surf. Sci. Catal.* **106**, 561 (1997).
5. Zhang, A., Nakamura, I., Aimoto, K., and Fujimoto, K., *Ind. Eng. Chem. Res.* **34**, 1074 (1995).
6. Mills, G. A., Heinemann, H., Milliken, T. H., and Oblad, A. G., *Ind. Eng. Chem.* **45**, 134 (1953).
7. Weisz, P. B., and Swegler, E. W., *Science* **126**, 887 (1957).
8. Chu, H. Y., Rosynek, M. P., and Lunsford, J. H., *J. Catal.* **178**, 352 (1998).
9. Shishido, T., and Hattori, H., *J. Catal.* **161**, 194 (1996).
10. Hosoi, T., Shimadzu, T., Ito, S., Baba, S., Takaoka, H., Imai, T., and Yokoyama, N., "Successful Design of Catalysts," Prepr. Symp. Div. Petr. Chem., Am. Chem. Soc., 562, p. 99. Elsevier, Amsterdam, 1988.
11. Ohgoshi, S., Nakamura, I., and Wakushima, Y., *Stud. Surf. Sci. Catal.* **77**, 289 (1993).
12. Conner, W. C., Pajonk, G. M., and Teichner, S. J., *Adv. Catal.* **34**, 1 (1986).
13. Roland, U., Braunshweig, T., and Roessner, F., *J. Mol. Catal. A: Chemical* **127**, 61 (1997).
14. Ebitani, K., Konishi, H., and Hattori, H., *J. Catal.* **130**, 257 (1991).
15. Ebitani, K., Konno, H., Konishi, H., and Hattori, H., *J. Catal.* **135**, 60 (1992).
16. Hattori, H., Shishido, T., Tsuji, J., Nagase, T., and Kita, H., "Science and Technology in Catalysis." p. 93. Kodansha, Tokyo, 1994.
17. Fujimoto, K., Adachi, M., and Tominaga, H., *Chem. Lett.* 547 (1985).
18. Roland, U., Winkler, H., Bauch, H., and Steinberg, K. H., *J. Chem. Soc., Faraday Trans.* **87**, 3921 (1991).
19. Roland, U., Salzer, R., and Summchen, L., *Stud. Surf. Sci. Catal.* **97**, 459 (1995).
20. Roessner, F., Roland, U., and Braunschweig, T., *J. Chem. Soc., Faraday Trans.* **91**, 1539 (1995).
21. Guisnet, M., Magnoux, P., and Martin, D., *Stud. Surf. Sci. Catal.* **111**, 319 (1997).
22. Hughes, T. R., and White, H. M., *J. Phys. Chem.* **71**, 2192 (1967).
23. Eberly, P. E., *J. Phys. Chem.* **72**, 1042 (1968).
24. Vedrine, J. C., Aurox, A., and Bolis, V., *J. Catal.* **59**, 248 (1979).
25. Zhang, A., Nakamura, I., and Fujimoto, K., *Stud. Surf. Sci. Catal.* **112**, 391 (1995).
26. Zhang, A., Nakamura, I., and Fujimoto, K., *J. Catal.* **168**, 328 (1997).
27. Fan, Y., Nakamura, I., and Fujimoto, K., *Stud. Surf. Sci. Catal.* **112**, 319 (1997).
28. Ueda, R., Tomishige, K., and Fujimoto, K., *Catal. Lett.* **57**, 145 (1999).
29. Jacobs, P. A., and Utterhoeven, J. B., *J. Chem. Soc., Faraday Trans. 1* **69**, 359 (1973).